

physical laws by more general geometrical concepts. A point (particle) is not only described by its four space-time coordinates, but director(s) have to be attached to each point. Therefore coordinate transformation would not only have to take the points into account, but also the director(s). These director(s) contain additional

physical information. They constitute a preferred direction (or directions), and so are violating the special principle or relativity on a micro-scale. Symmetry operations in these more general spaces become also more complex. For example, in this model one would not generally have invariance under reflection.

PHYSICAL REVIEW

VOLUME 159, NUMBER 5

25 JULY 1967

Multiple Meson Production by Heavy Primary Nuclei of Cosmic Origin and their Fragmentation Products at Energies above 10^{12} eV*

F. ABRAHAM, J. GIERULA,† R. LEVI SETTI, K. RYBICKI,† AND C. H. TSAO
*The Enrico Fermi Institute for Nuclear Studies and Department of Physics,
 The University of Chicago, Chicago, Illinois*

AND

W. WOLTER†
Institute of Nuclear Research, Krakow, Poland

AND

R. L. FRICKEN‡ AND R. W. HUGGETT
Department of Physics and Astronomy, Louisiana State University, Baton Rouge, Louisiana
 (Received 10 May 1965; revised manuscript received 6 March 1967)

Studies were made of the interactions initiated by fragments, including nucleons, from the gradual breakup of ultra high-energy heavy nuclei in a large block of nuclear emulsion. The results obtained by this approach are free from the detection biases that arise in scanning for, e.g., high-energy electromagnetic cascades. For one family of genetically related interactions the primary per-nucleon energy could be reliably established as ~ 1.3 TeV. The sample of nucleon-induced interactions with average multiplicity $n_s < 25$, with primary energies in the region of 1 TeV, show strong bimodality in the angular distribution of the created particles. An upper limit of 1.5 BeV/c is found for the average transverse momentum of the possible fireballs that could have given rise to this bimodality. The average inelasticity for the same sample of collisions is ~ 0.6 . The average multiplicity n_s for the nucleon-induced interactions with $N_h \leq 5$ is ~ 11.5 . For the interactions initiated by heavy nuclei the lower limit to the average per-nucleon multiplicity, $n_s/\Delta A$, in the energy interval 1–20 TeV is consistent with the average multiplicity for the nucleon-induced interactions at about 1 TeV. A linear superposition, in nucleus-nucleus collisions, of elementary nucleon-nucleon acts of meson production is suggested.

INTRODUCTION

THE purpose of the present investigation is the study of multiple meson production in the TeV region using the detailed information obtained from the collisions of heavy primary nuclei of the cosmic radiation in a large nuclear emulsion block. In the collision with an emulsion nucleus, a primary heavy nucleus can dissociate into fragments and/or single nucleons. The nuclear interactions of the latter can be observed provided the dimensions of the detector are large compared

with the collision mean free path in nuclear emulsion (~ 37 cm). A primary heavy nucleus thus initiates a family or cascade of interactions, and it is plausible to expect that those caused by multiply-charged fragments are due to incident nuclei carrying the same per-nucleon energy as the parent primary nucleus. Some of the nucleon fragments as well may emerge from the original fragmentation with energy close to the per-nucleon energy of the heavy primary. However, the remainder of the fragmentation products will be represented by nucleons which have lost energy after having been involved in the production of mesons in the first collision. As a result, the breakup of a heavy primary nucleus is expected to give rise to a beam of fragments and nucleons, with some spread in energy but with a well-defined "hard edge" of the per-nucleon energy which will correspond to that of the primary heavy nucleus.

* Research supported by the National Science Foundation and the U. S. Office of Naval Research.

† On leave from the Institute of Nuclear Research, Krakow, Poland. Present address: Instytut Badan Jodrowych, Krakow, Poland.

‡ National Science Foundation Graduate Fellow. Present address: Research Division, U. S. Atomic Energy Commission, Germantown, Maryland.

The advantages of such a situation are numerous and will be illustrated here. After giving the details of the exposure, scanning and representation of the data in Sec. 1, a family of interactions initiated by a phosphorus nucleus will be described in Sec. 2. The estimate of the primary energy, often difficult for individual jets, will be based instead on the observation of several energy-related interactions and, therefore, particularly reliable. Furthermore, the angular distributions of the particles created in nucleon-induced interactions, will be studied in a bias-free sample, such as obtained from along-the-track scanning of the breakup products. Thus it will be meaningful, in this sample, to search for effects due to specific mechanisms of meson production, and to investigate the inelasticities of the interactions, having available their entire spectrum. Section 3 deals with the analysis of several other nuclear fragmentation families initiated by nuclei of $Z \leq 7$, where, therefore, only a small number of interactions of nucleon fragments are available for each family. The observed multiplicities of meson production for interactions initiated by nucleons in the 1-TeV region and by heavy nuclei in the region of 1-20 TeV/nucleon are summarized in Sec. 4. Preliminary results of this investigation were reported.¹ Final results and some additional analysis were also reported.²

1. EXPERIMENTAL DETAILS

A. Exposure and Stack Properties

For the purpose of collecting a sample of interactions of heavy nuclei in conditions suitable for analysis as outlined above, a large emulsion block (80 liters) was flown from Brawley, California, in November, 1961.

The use of such large emulsion detectors for the study of ultra high energy interactions in the cosmic radiation was originally advocated by the late Schein.

The present stack consisted of 500 pellicles, $0.06 \times 45 \times 60$ cm³ in size, of Ilford K-5 emulsion. It was flown for 36 hs. at an almost constant altitude of 106 000 ft. (The flight curve is given in Ref. 3.) Alignment of the pellicles was achieved by x-ray markings. Before processing the pellicles were glass-mounted. Processing of the stack was accomplished within one month after the flight in Ryerson Physical Laboratory at the University of Chicago. After a preliminary visual scan of the plates,

¹ F. Abraham, C. L. Deney, R. L. Fricken, R. W. Huggett, J. Kidd, M. Koshiba, R. Levi Setti, C. H. Tsao, and W. Wolter. Presented at the Conference on Ultra High-Energy Nuclear Physics, Bristol, January 1963; EFINS Report No. 62-76. (unpublished).

² F. Abraham, J. Gierula, R. Levi Setti, K. Rybicki, C. H. Tsao, W. Wolter, R. L. Fricken, and R. W. Huggett, in *Proceedings of the Twelfth International Conference on High Energy Physics, Dubna, 1964* (Atomizdat, Moscow, 1966), p. 163. F. Abraham *et al.*, in *Proceedings of the Ninth International Conference on Cosmic Rays, London, 1965* (The Institute of Physics and The Physical Society, London, 1966), Vol. 2, p. 844. F. Abraham *et al.*, EFINS Report No. 65-44 (unpublished).

³ F. Abraham, J. Kidd, M. Koshiba, R. Levi Setti, C. H. Tsao, and W. Wolter, *Nuovo Cimento* **28**, 221 (1963).

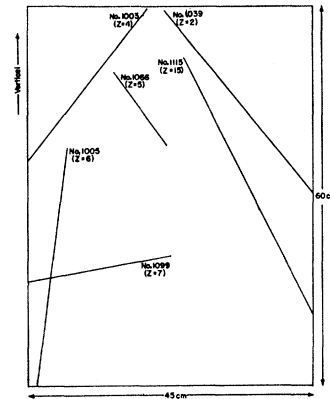


FIG. 1. Map, in the emulsion plane, of the 6 events described in the present paper.

each plate was cut into 12 pieces 15×15 cm² in size. The processed emulsion, of good transparency, had a plateau grain density of ~ 18 grains/100 μ .

B. Scanning Procedure and Measurements

Electromagnetic cascades were located by naked-eye scanning and were traced to their origins. Six events initiated by heavy primary nuclei ($Z \geq 2$) and with a path length per plate longer than 2 mm were found in the 60 liter part of the stack available to our laboratories. The location of the 6 events in the stack are shown in Fig. 1. Each event is represented by a line which extends from the point of the primary interaction to the point the shower left the stack. Careful scanning along these lines for the interactions of nuclear fragments were performed as follows: (a) All fragments of $Z \geq 2$, were traced to where they interacted or left the stack. (b) In order to isolate fragments of $Z = 0, 1$ from

TABLE I. Charges of the primary nuclei and heavy fragments ($Z \leq 3$), as determined from δ -ray counting.

Event No.	Type of interaction	Charge of the primary (from δ rays)
1003-1	(5+37+ α)Be	4.2 \pm 0.5
1003-2	(23+95) α	
1005-1	(13+215)C	6.0 \pm 0.4
1039-1	(0+24+ α) α	
1039-2	(1+47) α	
1066-1	(2+1+B)B	5.2 \pm 0.4
1066-3	(24+179)B	4.9 \pm 0.4
1099-1	(0+10+C)N	7.1 \pm 0.4
1099-2	(1+54+2 α)C	5.7 \pm 0.4
1115-1	(3+7+Mg)P	15.1 \pm 0.6
1115-2	(11+42+Na)Mg	12.3 \pm 0.9
1115-5	(0+3+Na)Na	11.2 \pm 0.5
1115-13	(1+4) α	
1115-20	(0+44)Li	

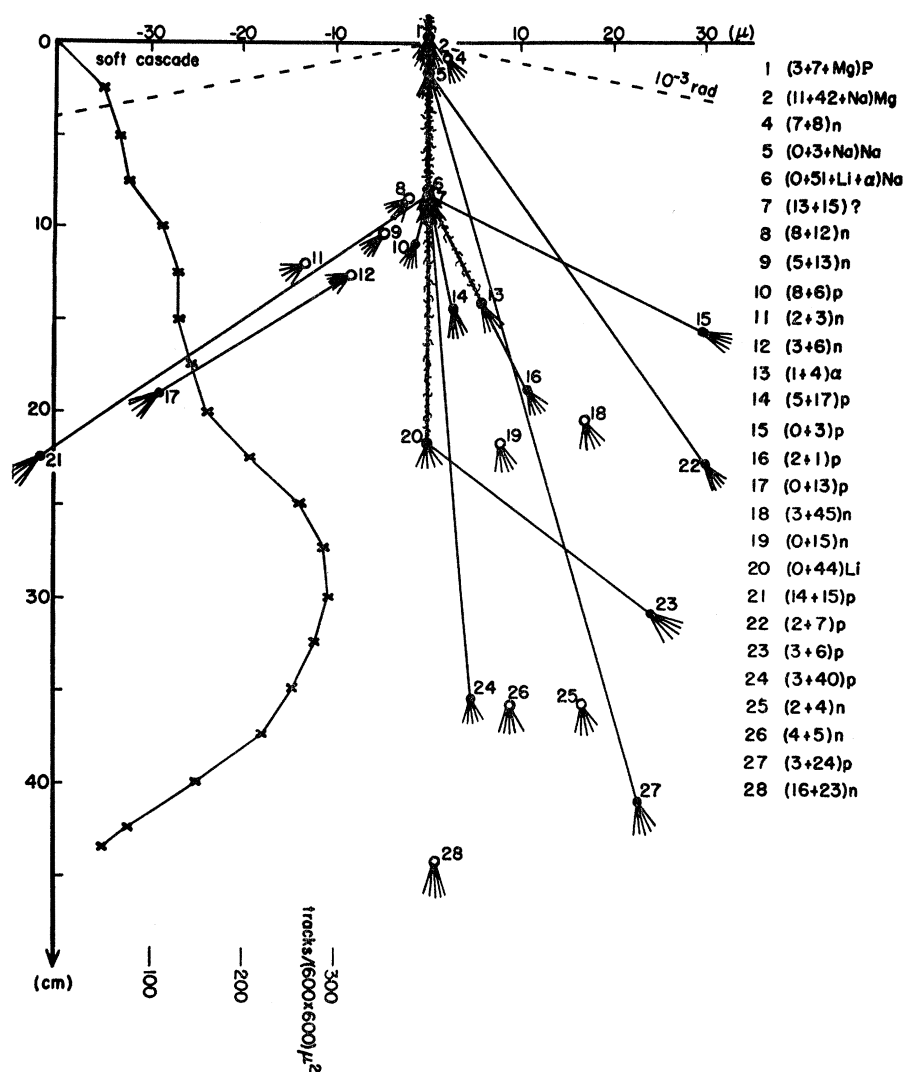


FIG. 2. Map, in the emulsion plane, of the development of family No. 1115 (for $\theta < 1$ mrad) and accompanying electromagnetic cascade. The event type is described by the notation $(A+B+C)D$, where A is the number of secondaries at plateau ionization, B the number of gray and black tracks, C if any, indicates the nature of outgoing fragments of $Z \geq 2$, and D the nature of the incoming primary particle.

the background of created particles, an estimate of Z for the parent nucleus was first obtained. With this information, the approximate number of $Z=0, 1$ fragments to be found could be anticipated. An attempt was then made to follow individually the anticipated number of singly-charged fragments having the smallest emission angles. By this approach an angular region was defined in which to scan for the interactions of neutron fragments. For the events considered here, such a region was found to be typically smaller than 10^{-3} rad.

Whenever following of individual tracks was not possible due to the dense electromagnetic cascade, area scanning was performed for all high-energy interactions which could have been caused by neutral or singly-charged fragments.

It should be emphasized that the sample of jets induced by singly-charged fragments, which ensued from such along-the-track scanning, is unbiased as to the jet topology.

The emission angles of all secondaries were measured for both the primary heavy nucleus and the fragment interactions. This could be done with particular accuracy ($\sim 10^{-5}$ rad) whenever a $Z \geq 2$ fragment survived the first breakup and thus defined the shower axis.

The charges Z of all primary nuclei and heavy fragments ($Z \geq 2$) were measured by δ -ray counting. The measured charges are given in Table I. The development of the electromagnetic cascade accompanying each family of interactions was determined by measuring the electron density as a function of the depth in the shower.

C. Representation of the Data

The experimental information on which this investigation is mostly based is provided by the production angular distributions of shower particles measured in the laboratory frame of reference. It is convenient to analyse such data by using $\log_{10} \tan \theta$ as a variable, where θ is the emission angle relative to the direction of the in-

coming particle. As is well known, this variable yields an estimate of the primary energy according to the Castagnoli relation⁴

$$-\log_{10}\gamma_c = \langle \log_{10} \tan\theta \rangle \quad (1)$$

which holds within the region of validity of restrictive approximations. (γ_c is the Lorentz factor of the barycentric system of colliding nucleons, γ_{cp} , γ_{cs} , in the following will refer to the primary collision or to collisions generated by jet secondaries, respectively). A very useful property of this variable is that the shape of its distribution is identical with that of the distribution of $\log_{10} \tan\frac{1}{2}\theta^*$, where θ^* is the emission angle of the secondary particles in *any* system moving with respect to the laboratory system with a sufficiently large Lorentz factor ($\gamma \gg 1$)⁵ The $\log_{10} \tan\theta$ distributions for the events studied here will be presented in ideogram form (see, e.g., Figs. 3, 8-12), each track being represented by a rectangle having a constant base $\Delta \log_{10} \tan\theta = 0.4$ (as a rule larger than the measuring errors) and a constant height.

2. THE FAMILY OF NUCLEAR INTERACTIONS INITIATED BY A $Z=15$ PRIMARY NUCLEUS (EVENT NO. 1115)

Event No. 1115 is the most informative family of interactions. Its development in the stack is schematically described in Fig. 2, while the $\log_{10} \tan\theta$ plots of the events chosen for investigation are given in Fig. 3.

A. Identification of Nucleon Fragments

The charge of the primary nucleus is $Z=15$. The primary nucleus and its heavy ($Z \geq 2$) fragments produced 7 interactions in the stack. Since the potential length of the event in the stack is 45 cm, there is a large probability that many of the approximately 30 nucleons emerging from the heavy-nucleus interactions will in turn interact in the stack.

Seventeen singly-charged particles were emitted from the 7 heavy fragment interactions at angles smaller than 10^{-3} rad. As seen in Fig. 3, these particles form a "core" (inner cone) which is well separated from the shower tracks appearing at greater angles (outer cone). This feature and the multiplicity in the group, which is close to the number of protons in the primary nucleus ($Z=15$), strongly suggest that these tracks are due to protons emerging from the successive breakups of the primary nucleus. This hypothesis can be checked by calculating the expected number of interactions caused by 31 nucleons (the most probable A for a nucleus with $Z=15$) originating from the primary nucleus and comparing this number with the number of core-particle

⁴ C. Castagnoli, G. Cortini, C. Franzinetti, A. Manfredini, and D. Moreno, Nuovo Cimento 10, 1539 (1953).

⁵ J. Gierula, Fortschr. Physik 11, 109 (1963).

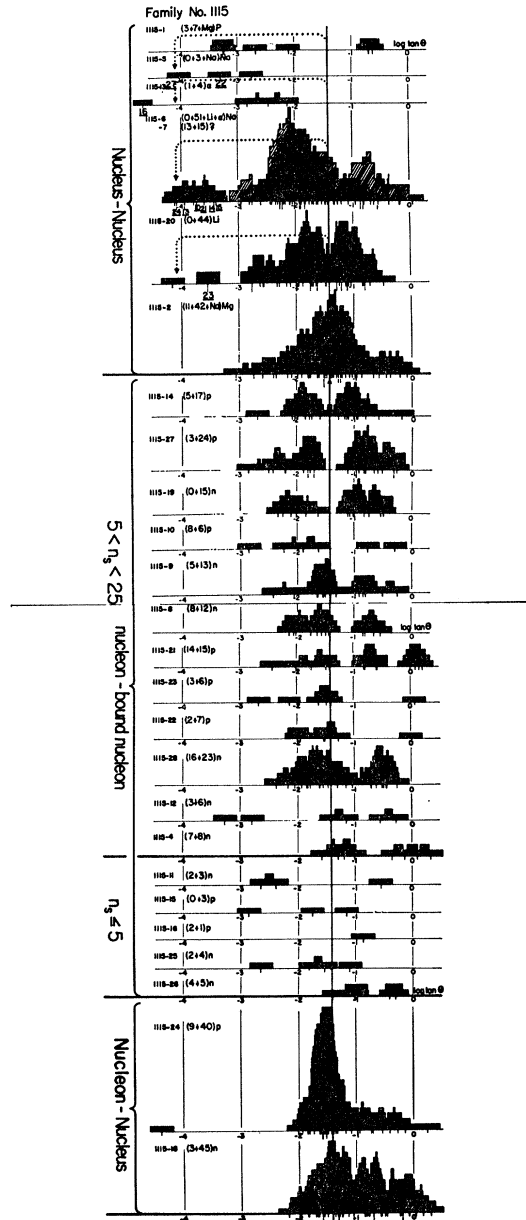


FIG. 3. $\log_{10} \tan\theta$ plot of the particles produced in each of the jets associated with family No. 1115. The first six distributions refer to $Z \geq 2$ interactions. The vertical line indicates the best estimate of the $\log_{10} \gamma_{cp}$ value for the primary nucleons (γ_{cp} is the Lorentz factor of the barycentric system of colliding nucleons). The dotted lines on the first four distributions indicate the $\log_{10} \tan\theta$ values for breakup nucleons as predicted by the Kaplon relation [Ref. 10]. The marks below the abscissas indicate the $\log_{10} \tan\theta$ values for individual tracks. The vertices of events 1115-6 and 7 are only 100μ apart, and therefore the two angular distributions could not be completely resolved. The shaded ideogram is the best estimate of the distribution belonging to the event 1115-7.

interactions actually observed. (The charges of all heavy fragments are given in Table I and Fig. 2.) The number of protons which were separated from the incident heavy nucleus in a given interaction should equal

TABLE II. $\log_{10}\gamma_{cs}$, σ and $\log_{10}K_{ch}$ values for the fragment-nucleon interactions with $5 < n_s < 25$.

Event No.	Type of interaction	$\log_{10}\gamma_{cs} \pm \frac{\sigma}{\sqrt{n_s}}$	σ	$\log_{10}K_{ch}$
1115-14	(5+17) <i>p</i>	1.41 ± 0.15	0.64	-0.38 ± 0.34
1115-27	(3+24) <i>p</i>	1.33 ± 0.16	0.77	0.01 ± 0.34
1115-19	(0+15) <i>n</i>	1.30 ± 0.17	0.66	-0.23 ± 0.31
1115-10	(8+6) <i>p</i>	1.61 ± 0.39	0.94	-0.91 ± 0.86
1115-9	(5+13) <i>n</i>	1.31 ± 0.17	0.62	-0.44 ± 0.36
1115-8	(8+12) <i>n</i>	1.42 ± 0.16	0.57	-0.60 ± 0.34
1115-21	(14+15) <i>p</i>	0.89 ± 0.24	0.87	0.32 ± 0.53
1115-23	(3+6) <i>p</i>	1.55 ± 0.38	0.92	-0.96 ± 0.83
1115-22	(2+7) <i>p</i>	1.38 ± 0.30	0.73	-0.83 ± 0.61
1115-28	(16+23) <i>n</i>	1.28 ± 0.13	0.64	-0.14 ± 0.34
1115-12	(3+6) <i>n</i>	1.59 ± 0.49	1.21	-0.84 ± 1.17
1115-4	(7+8) <i>n</i>	0.65 ± 0.25	0.71	0.14 ± 0.53

the change ΔZ in the charge Z of the interacting nucleus. Assuming for the separated neutrons the same distribution of potential lengths in the stack as observed for the singly-charged fragments, it is found that out of 31 nucleons separated successively from the primary nucleus and its heavy fragments, approximately 19-20 would be expected to interact in the stack. Of these, roughly half should be protons (with a possible deuteron or triton contamination) and the other half, neutrons. The possible pion contamination amongst the charged core-particles was estimated from the ratio of solid angles subtended by the tracks in the inner and outer cones, respectively, and found not to exceed 10%.

The systematic following of all 17 tracks in the core and a very careful area scanning of the core cone yielded 9 interactions caused by charged particles and 10 interactions caused by neutral particles. This result is consistent with the hypothesis that all of the particles appearing in this family at angles smaller than 10^{-3} rad indeed correspond to breakup nucleons.

B. Estimate of the Primary Energy

The primary energy of the nucleus initiating family No. 1115 can be estimated from a study of both the nucleon-induced and the heavy-fragment-induced core-particle interactions. While the fragments of $Z \geq 2$ should carry the same per-nucleon energy as the primary nucleus, this may not, in general, be the case for the breakup nucleons. In fact, since ~ 150 mesons were produced in addition to the core-particles in the 7 successive breakups of multiply-charged fragments, one can very roughly estimate that only about one-half of the nucleons composing the primary heavy nucleus did not interact. Therefore, one should expect the secondary interactions of the singly-charged particles (*p* events) and the neutrals (*n* events) in the cone of opening angle 10^{-3} rad to exhibit some spread in energy up to an edge corresponding to the true primary energy. Using the Castagnoli method for estimating primary energies, the

detection of the hard edge will be possible only for a special kind of collision. One of the most restrictive requirements for the validity of the method is, in fact, that of fore-aft symmetry among the shower particles produced. Furthermore since, given γ_c , the primary energy estimate depends on the generally unknown target mass by the relation

$$E_p \approx 2M_T \gamma_c^2, \quad (2)$$

where M_T is the target mass, it will be advisable to search for a hard edge only amongst those interactions which are most likely nucleon-nucleon collisions. Thus amongst the core-particle interactions one should select (a) those showing a clear fore-aft symmetry of shower particle emission, or more generally, any feature apt to identify the abscissa of the center of collision (in the $\log_{10} \tan \theta$ scale); (b) the most likely nucleon-nucleon, or nucleon-bound-nucleon collisions. To satisfy the latter condition it was required that the multiplicities n_s be less than 25. No events with $n_s < 6$ have, on the other hand, been included in the analysis of the primary energy, since a meaningful estimate of γ_c cannot be obtained from the angular distributions of such events. The first 12 *p* and *n* events in Fig. 3 fulfilled these criteria. The values of $\log_{10} \gamma_{cs}$ for these jets, as derived from (1), are given in Table II, and can be seen, with the exception of two events (1115-21 and 1115-4), to lie within rather narrow limits. Among the $\log_{10} \gamma_{cs}$ values of better statistical significance, the upper edge can be placed at $\log_{10} \gamma_{cs} \approx 1.4$. It was furthermore observed that the majority of the 12 *p* and *n* events show a very pronounced dip in the central part of the angular distribution, which divides the distribution itself in two nearly equal groups of tracks. This feature which indicates a strong forward-backward anisotropy of particle emission in the barycentric system of the colliding nucleons also provides additional information helpful in identifying the $\log_{10} \tan \theta$ value corresponding to the center of collision. In fact, it is felt that such identification may be less dependent on fluctuations of the relative numbers of particles emitted forward or backward, than that provided by the Castagnoli method. Thus, the ordering of these events in Fig. 3 and Table II is made according to the location of the characteristic dips. On this basis, the hard edge is once again placed at a value of $\log_{10} \gamma_{cs} \approx 1.42$ or per-nucleon energy of the primary nucleus of ≈ 1.30 TeV. This $\log \gamma_{cs} = \log \gamma_{cp}$ value is indicated by a vertical line drawn through the whole family of histograms in Fig. 3.

Is this estimate of the primary per nucleon energy consistent with the information which can be directly derived from the interactions of the multiply-charged fragments themselves? One can see that the mode of the only symmetric angular distribution (event No. 1115-2) overlaps the edge line. On the other hand, event No. 1115-20 shows a bimodal asymmetric distribution, the valley of which overlaps this line, and it is tempting

once again to identify the location of the valley with the center of collision. It is worthwhile to point out that the shape of the angular distribution of this nucleus-nucleon interaction is similar to the "mirror system" shapes observed in nucleon-nucleus collisions having similar multiplicities.⁶ The collision involved, $(0+44)\text{Li}$, could then be a nucleus-nucleon collision. (It is difficult to imagine in such a case the absence of evaporation tracks from the target nucleus were it not a hydrogen nucleus.) Event No. 1115-6, of the type $(0+51+\alpha, \text{Li})\text{Na}$ seems to be another example of this kind of collision (in which the Castagnoli relation would give an overestimate of the primary energy.) Since there are many indications that in nucleon-nucleus collisions (the mirror case) the Castagnoli method underestimates the true energy,⁷⁻⁹ and since the corresponding angular distributions are strongly asymmetric, these observations are not inconsistent with the above energy estimate obtained from symmetric collisions.

The well-separated small-angle nucleons emerging from the partial fragmentations provide confirmation of the above primary energy estimate. If these nucleons were not involved in the production of mesons, but only evaporated from the incident nucleus, then they should appear at a mean angle $\langle\theta\rangle$ corresponding to the formula¹⁰

$$\langle\theta\rangle \cong \frac{0.12}{E_p(\text{GeV})}, \quad (3)$$

where E_p is the energy per nucleon of the incident nucleus. As shown by a dotted line in Fig. 3 some of the core nucleons (the hard edge) appear in the angular region predicted by the above relation (3), when $E=1.30$ TeV. The majority of the particles, however, are observed at larger angles. A plausible explanation of this shift is that several of the core particles correspond to nucleons which took part in meson production during the fragmentation process.

Now let us consider the remaining 7 p and n events which have not yet been discussed. Among them there are two large-multiplicity collisions, event No. 1115-24 $(9+40)p$ and event No. 1115-18 $(3+45)n$. Both show very asymmetric angular distributions, high multiplicities, and several evaporation tracks. These features suggest that these are collisions involving more than one nucleon of the target nucleus and, therefore, seem to preclude the obtaining of a reliable energy estimate from these two events. None of the low-multiplicity events

(see Fig. 3, $n_s \leq 5$) are very informative concerning primary energy, but they are consistent with the energy estimate given above.

For reference in the following, the primary per nucleon energy of event No. 1115 will be taken as 1.3 TeV corresponding to $\log_{10}\gamma_{ep}=1.42$.

A conservative estimate of the error on this value, obtained by combining the errors on $\log_{10}\gamma_c$ from the symmetric event No. 1115-2 and from the first three events corresponding to the high-energy edge (No. 1115-14, -27 and -19) is $\Delta \log_{10}\gamma_{ep} = \pm 0.06$.

C. The Angular Distribution of Particles Produced in the Interactions of Nucleon Fragments

Nineteen interactions produced by p and n primaries in this family were found as described above, by systematic following of tracks of singly-charged particles and by systematic area scanning for neutral interactions. Therefore, these 19 interactions represent an unbiased sample of interactions caused by nucleons with energies in the region 1.3 TeV and below. This situation is unprecedented and is of particular value in giving a reliable picture of the angular distribution of produced secondaries at this energy. As seen in Fig. 3 the angular distributions for the majority of the interactions which can be interpreted as being nucleon-nucleon collisions indicate a striking bimodal structure. This has been observed as a frequent feature of high-energy nucleon-nucleon collisions in many investigations.¹¹⁻¹⁴ The occurrence of bimodal angular distributions (together with the observed independence of the transverse momenta on the primary energy) was the basic motivation for proposing the fireball model of multiple meson production.^{11,12,15,16} According to this model, secondary particles are emitted isotropically from two independent centers moving (in opposite directions) with respect to the center-of-mass system of the colliding nucleons. In the $\log_{10} \tan\theta$ coordinate, the angular distribution consists of 2 Gaussians, each with dispersion $\delta \approx 0.36$, where the separation between the two maxima is a function of the Lorentz factor of the two fireballs with respect to the center of collision.

Czyzewski and Krzywicki¹⁷ suggested a modified statistical model of multiple meson production which predicts a quasirectangular angular distribution in the $\log_{10} \tan\theta$ variable. In their opinion this model offers a

⁶ J. Gierula, R. Hołyński, and M. Mięśowicz, in *Proceedings of the International Conference on Cosmic Rays and the Earth Storm, Kyoto, 1961* (The Physical Society of Japan, Tokyo, 1962), Vol. 3, p. 405.

⁷ E. Lohrmann, M. W. Teucher, and Marcel Schein, *Phys. Rev.* **122**, 672 (1961).

⁸ A. Barbaro-Galtieri, G. Baroni, A. Manfredini, C. Castagnoli, C. Lamborizio, and I. Ortalli, *Nuovo Cimento* **20**, 487 (1961).

⁹ J. Gierula (unpublished).

¹⁰ M. F. Kaplon, B. Peters, H. L. Rynolds, and D. M. Ritson, *Phys. Rev.* **85**, 295 (1952).

¹¹ P. Ciok, T. Coghen, J. Gierula, R. Hołyński, A. Jurak, M. Mięśowicz, T. Saniewska, O. Stanis, and J. Pernegr, *Nuovo Cimento* **8**, 166 (1958).

¹² P. Ciok, T. Coghen, J. Gierula, R. Hołyński, A. Jurak, M. Mięśowicz, T. Saniewska, and J. Pernegr, *Nuovo Cimento* **10**, 741 (1958).

¹³ J. Gierula, M. Mięśowicz, and P. Zieliński, *Nuovo Cimento* **18**, 102 (1960).

¹⁴ J. Gierula, D. M. Haskin, and E. Lohrmann, *Phys. Rev.* **122**, 626 (1961).

¹⁵ G. Cocconi, *Phys. Rev.* **111**, 1699 (1958).

¹⁶ K. Niu, *Nuovo Cimento* **10**, 994 (1958).

¹⁷ O. Czyzewski and A. Krzywicki, *Nuovo Cimento* **30**, 603 (1963).

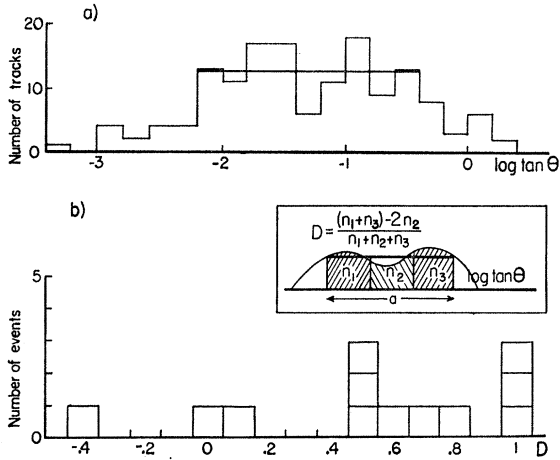


FIG. 4. (a) Composite angular distribution of particles produced in the interactions of core nucleons. The horizontal line is the best fit (neglecting the tail ends) for a rectangular distribution. (b) Frequency distribution of the ratio $D = (n_1 + n_3 - 2n_2) / (n_1 + n_2 + n_3)$. See insert for the definitions of n_1 , n_2 , and n_3 .

better fit to the old experimental data than the fireball model. The present data, on the other hand, is in strong contradiction with such a model. The shape of the angular distributions significantly deviate, in the majority of cases, from the rectangular one and in the direction predicted by the fireball model.

The significance of the discrepancy was tested in two ways: (1) All the distributions in the laboratory system, which could be interpreted as being due to nucleon-nucleon collisions, were added and the composite distribution compared with a rectangular distribution. Because the linear shift (along the $\log_{10} \tan \theta$ axis) of individual $\log_{10} \tan \theta$ distributions caused by the energy spread in our beam of nucleons is not very large, such a composite distribution should not destroy the characteristics of the individual distributions. This is shown in Fig. 4a where the horizontal line represents the best fit (neglecting the tails) to a rectangular distribution. The composite histogram retains a symmetric bimodal shape which deviates from the rectangular distribution by two standard deviations according to the χ^2 test. This test, however, does not take into account the fact that the deviation from a rectangular distribution is consistently observed to occur near the central value of the distribution. Thus, another test was introduced. (2) Each individual distribution was approximated by the best fit to a rectangular distribution as illustrated in the insert of Fig. 4(b), by making the area of the ideogram above the horizontal line equal to the "missing area" below the line. The range a of the distribution was then divided into 3 equal parts containing n_1 , n_2 , and n_3 tracks, respectively. For a rectangular distribution $n_1 = n_2 = n_3$. Thus, the ratio

$$D = \frac{(n_1 + n_3) - 2n_2}{n_1 + n_2 + n_3} \quad (4)$$

TABLE III. Partial multiplicity in equal angular intervals for the fragment-nucleon interactions ($5 < n_s < 25$).^a

Interaction No.	Type of interaction	n_1	n_2	n_3	$n_1 + n_2 + n_3$	D
1115-14	(5+17) p	5	1	6	12	+0.75
1115-27	(3+24) p	6	1	7	14	+0.78
1115-19	(0+15) n	4	4	6	14	+0.14
1115-10	(8+6) p	2	2	2	6	0
1115-9	(5+13) n	2	6	5	13	-0.38
1115-8	(8+12) n	5	0	3	8	+1.00
1115-21	(14+15) p	2	0	4	6	+1.00
1115-23	(3+6) p	3	0	1	4	+1.00
1115-22	(2+7) p	4	1	1	6	+0.50
1115-28	(16+23) n	8	3	7	18	+0.50
1115-12	(3+6) n	2	1	3	6	+0.50
1115-4	(7+8) n	3	1	3	7	+0.57
Total number		46	20	48	114	

^a See the text and Fig. 4(b) for the definitions of n_1 , n_2 , n_3 , and D .

for a rectangular distribution is expected to fluctuate around zero. For a bimodal distribution, on the other hand, the expected values of D should be predominantly positive with a maximum value of unity. Figure 4(b) shows the distribution of D values for the 12 interactions believed to be nucleon-nucleon collisions. Low-multiplicity events have been omitted since they give little information concerning the shape of the distribution. The distribution is grossly inconsistent with symmetry around zero. Table III shows values of n_1 , n_2 , n_3 , and D for the individual jets. The χ^2 test applied to the sums of n_1 , n_2 , n_3 indicates that the observed sample deviates from the rectangular distribution by more than three standard deviations.

D. Angular Distribution of Particles in the Outer and Inner Shower Cones

A critical point in connection with the fireball model is the requirement that particles should be emitted isotropically in the rest frames of the fireballs. A check of this requirements is provided by the Duller-Walker plots which have been constructed separately for the forward and backward cones of the 12 nucleon-nucleon jets investigated in the previous section (Fig. 5). The distributions are consistent with isotropic emission within the limits of approximately one standard deviation.

E. Azimuthal Angular Distributions of Particles Produced in the Interactions of Nucleon Fragments

A further question of interest in connection with the fireball model is the direction of motion of the fireballs. In the simplest model¹² it has been assumed that the fireballs move along an axis defined by the direction of the incident nucleon. A divergence from this axis might be reflected in a deviation of the azimuthal angles from isotropy. Quite independently of any particular model the existence of such anisotropy would clearly

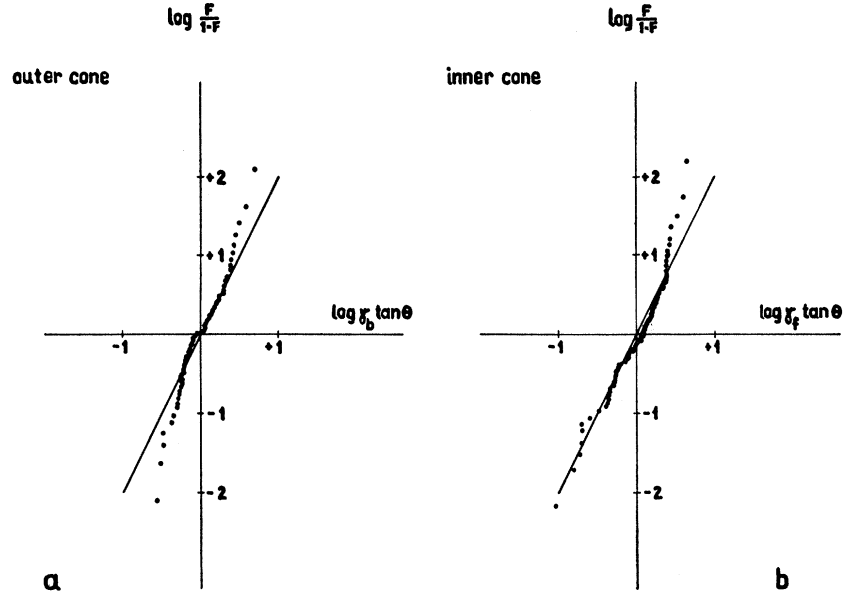


FIG. 5. The Duller-Walker plots of shower particles from (a) the outer and (b) the inner cones of 12 probable nucleon-nucleon collisions produced by breakup nucleons in family No. 1115. Straight lines in the diagrams correspond to isotropic distributions.

indicate particle emission from two separate centers, rather than from a central interaction region.

The presence of multiply-charged fragments in family No. 1115 enables the direction of the primary particle to be determined with a precision of the order of 10^{-5} rad. As a result, the azimuthal angles for all secondary particles (including those which are most collimated) are unambiguously defined in these interactions. It is to be noted that in the majority of high-energy jet investigations, the direction of the primary particle is usually *assumed* to coincide with the centroid of the most collimated bundle of tracks. In the present investigation

this assumption has been checked experimentally and it appears to be verified within statistical errors.

The azimuthal angular distribution has been analyzed using the unit vector method suggested by Bogdanowicz

TABLE IV. Azimuthal asymmetry parameters for the produced particles of all the fragment-nucleon interactions with $n_s < 25$.

Interaction No.	Type of interaction	w	w_f	w_b
1115-4	(7+8) n	0.35	0.46	0.84
1115-8	(8+12) n	2.52	2.06	0.46
1115-9	(5+13) n	0.04	0.65	1.77
1115-10	(8+6) p	0.33	0.12	0.28
1115-11	(2+3) n	1.77	1.90	1.00
1115-12	(3+6) n	0.52	0.01	0.85
1115-14	(5+17) p	1.93	0.33	1.88
1115-15	(0+3) p	0.59
1115-19	(0+15) n	0.07	0.11	0.25
1115-21	(14+15) p	0.91	0.70	1.44
1115-22	(2+7) p	0.15	0.06	1.00
1115-23	(3+6) p	0.17	0.24	1.00
1115-25	(2+4) n	0.07
1115-26	(4+5) n	0.21	0.50	0.02
1115-27	(3+24) p	1.54	0.94	1.08
1115-28	(16+23) n	0.24	0.11	0.65

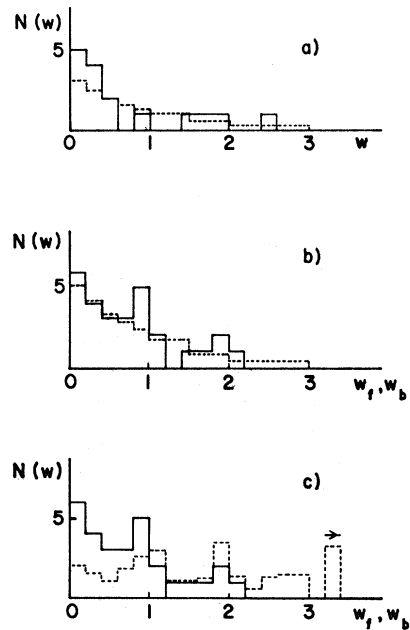


FIG. 6. (a) Frequency distribution of the azimuthal asymmetry parameter for jets induced by core nucleons. (The dotted line corresponds to a uniform azimuthal distribution.) (b) Similar distributions for the particles associated with a forward or a backward fireball for interactions exhibiting a "two-center" structure (merged into one distribution). (c) The experimental distribution of Fig. 6(b) as well as the distribution for corresponding artificial jets having $p_{FF} = 1.5$ BeV/c.

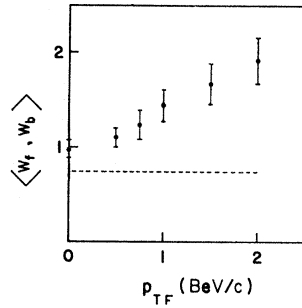


FIG. 7. The variation of the mean value of w_f and w_b with p_{TF} exhibited by artificial jets corresponding to the jets for which w_f and w_b have been measured. The measured value of 0.74 is indicated by the dashed line. The mean value of w_f and w_b corresponding to azimuthal symmetry and $p_{TF}=0$ is unity.

*et al.*¹⁸ Defining \mathbf{r} as the sum of the unit vectors along the projection of the charged secondary tracks in the azimuthal plane perpendicular to the direction of the primary axis, the value

$$w = |\mathbf{r}|^2/n_s \quad (5)$$

is then calculated for each jet. The probability distribution of w has the simple exponential form, $p(w)dw = e^{-w}dw$, if the distribution of azimuthal angles is uniform.¹⁸

The results of these calculations applied to the 16 jets, which can be interpreted as being nucleon-nucleon interactions, are presented in Table IV and Figs. 6(a), and (b). (This sample also contains 4 events with $n_s > 6$ which were not considered in the preceding analysis.) The w values were calculated using all secondaries of each jet, as well as the tracks in groups associated with a forward or a backward fireball in those jets exhibiting a "two-center" structure. (The latter are denoted as w_f and w_b , respectively.) As can be seen from Figs. 6(a), and 6(b), the hypothesis of a uniform distribution of azimuthal angles (dotted line) seems to be consistent with the experimental data.

Artificial two fireball jets were constructed with a high-speed computer to correspond to the group of jets used in this analysis. Distributions were obtained for w , w_f , and w_b for various values of fireball transverse momentum p_{TF} . The distribution of w was found to depend on p_{TF} only over a rather limited range, over which the deviation from the distribution of measured w values was not large enough to establish an upper limit for p_{TF} . The distribution of w_f and w_b , however, did show a definite shift toward higher values with increasing p_{TF} . See Fig. 6(c). This change in the distribution can be parameterized by the mean value of w_f and w_b , which is shown as a function of p_{TF} in Fig. 7. For $p_{TF}=1.5$ BeV/c the mean value of w_f and w_b is 1.67 which is approximately 3 standard deviations above the mean value of unity corresponding to the uniform

azimuthal distribution with $p_{TF}=0$, and more than 4 standard deviations above the measured mean value of 0.74. Taking $p_{TF}=1.5$ BeV/c as an upper limit for the fireball transverse momentum of the 14 jets which exhibited a "two-center" structure clearly excludes for primary energies around 1 TeV the average value of 3.9 ± 0.6 BeV/c which was found by Akashi *et al.* for 12 nuclear interactions with primary energies above 100 TeV.¹⁹

F. Inelasticity Coefficient in the Interactions of Nucleon Fragments

It has been customary to obtain from the angular distribution the energy radiated as charged particles E_{ch} by assuming that the mean transverse momentum for all secondaries is independent of angle and equal to ~ 0.4 GeV/c. Consequently,

$$E_{ch} \cong \sum_{i=1}^{n_s} \frac{0.4}{\sin \theta_i} \text{ GeV}. \quad (6)$$

For the events which show a clear bimodality, the fireball model yields the following alternative estimate:

$$E_{ch} = (n_{sf}\gamma_f + n_{sb}\gamma_b)0.5 \text{ GeV}, \quad (7)$$

where n_{sf} and n_{sb} are the number of tracks in the forward and backward group of tracks, respectively, and γ_f and γ_b are the Castagnoli estimates of the Lorentz factor in the laboratory system for the forward and

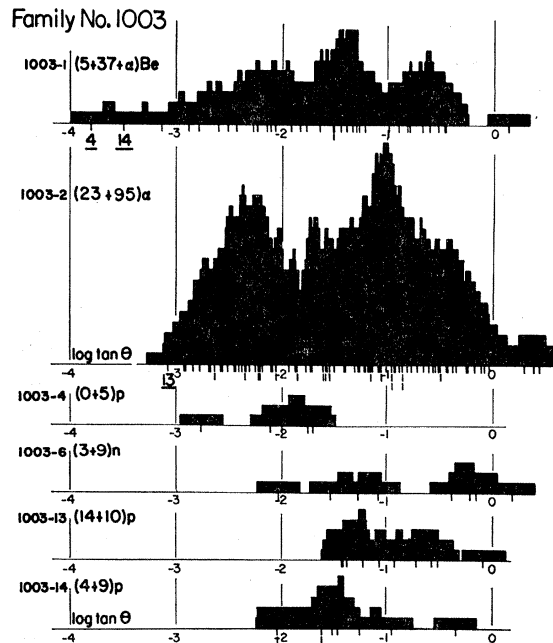


FIG. 8. $\log_{10} \tan \theta$ plot of the produced particles in the jets associated with family No. 1003.

¹⁸ J. Bogdanowicz, P. Ciok, Z. Galster, T. Saniewska, and P. Zieliński, Nucl. Phys. 40, 270 (1963).

¹⁹ M. Akashi *et al.*, in *Proceedings of the Ninth International Conference on Cosmic Rays, London, 1965* (The Institute of Physics and the Physical Society, London, 1966), Vol. 2, p. 835.

backward fireball, respectively. If one assumes isotropy of the pion angular distribution in the fireball rest system, 0.5 GeV represents the average total energy of a pion in the fireball rest system for $\langle p_i \rangle \approx 0.4$ GeV/c.

As a rule, the second term is much smaller than the first term and can be omitted. Relation (7) is less sensitive than (6) to the fluctuations of E_{ch} introduced by the presence of a very small angle track.

Values of E_{ch} have been calculated from Eq. (7) for the 12 interactions of Table II. The total inelasticity coefficients in these interactions were then obtained from

$$K_{ch} = 1.5E_{ch}/2M\gamma_{cs}^2, \quad (8)$$

where the factor 1.5 takes into account the π^0 contribution, assuming charge independence. We have chosen to define K_{ch} accordingly to (8), rather than as used previously by several authors, where K_{ch} represented the partial inelasticity into charged particles only. The errors of $\log_{10}K_{ch}$ have been taken according to (7) and (8) as

$$\left(\frac{\Delta K}{K}\right)^2 = (\Delta \log_{10}K)^2 = \frac{4\sigma_s^2}{n_s} + \frac{\sigma_f^2}{n_f}, \quad (9)$$

where σ_s^2 is the variance of the over-all $\log_{10} \tan\theta$ distribution, σ_f^2 is the variance of the $\log_{10} \tan\theta$ distribution of the forward group of tracks used for calculating E_{ch} , and n_f is the number of tracks in this group. The values of $\log_{10}K_{ch}$ are presented in Table II. The mean value of $\log_{10}K_{ch}$ corresponds to $\langle K_{ch} \rangle = 0.57_{-0.14}^{+0.19}$.

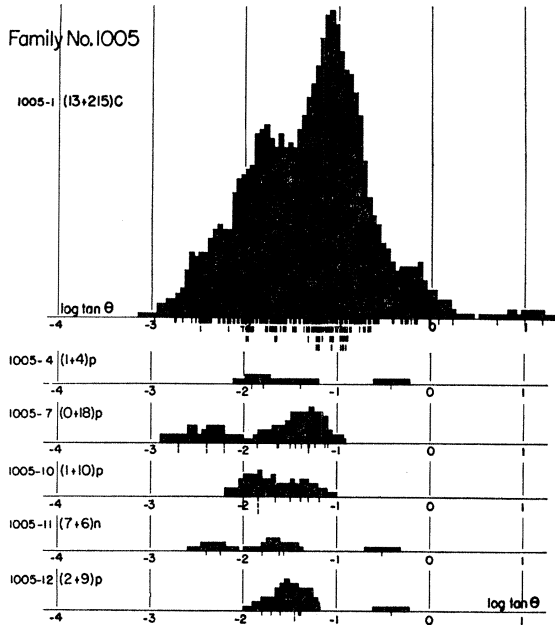


FIG. 9. $\log_{10}\tan\theta$ plot of the produced particles in the jets associated with family No. 1005.

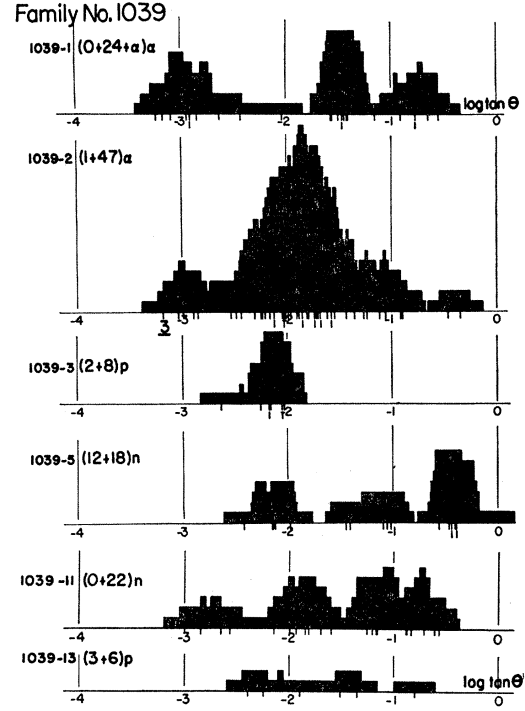


FIG. 10. $\log_{10}\tan\theta$ plot of the produced particles in the jets associated with family No. 1039.

3. ANALYSIS OF THE REMAINING NUCLEAR FRAGMENTATION FAMILIES

The remaining five families differ fundamentally from Event No. 1115, because (1) the charges of the primary nuclei are much smaller (2, 4, 4, 6, 7); (2) the respective potential lengths in the stack are shorter; (3) the primary nucleus is completely broken up into singly-charged or neutral fragments after the first or second interaction; in three cases (Nos. 1003, 1005, 1066) the target is a silver or bromine nucleus; (4) the dense electromagnetic cascade prevents the systematic following of individual tracks over the entire potential length. These features are apparent from an inspection of Figs. 1 and 8-12. As a consequence, much less can be said about the interactions of individual nucleons. However, the secondary interactions found in the area scanning along the electromagnetic cascade are still useful for obtaining estimates for the primary energy of the heavy nucleus, which are better than those derived from the angular distribution of the single primary interaction. Relevant information on these events is contained in Table V.

A. Energy Estimates

The primary energy per nucleon E_p in the five families was evaluated by combining the following information:

(1) The Castagnoli estimate of the primary energy from interactions of the heavy primary and its heavy

fragments. Here the shapes of the particular $\log_{10} \tan \theta$ distributions were examined and greater weight was given to estimates corresponding to symmetric shapes. In cases for which the $\log_{10} \tan \theta$ distribution exhibited an asymmetric shape, a check was made to see if the observed shift of the Castagnoli estimate could be understood as the consequence of an asymmetry in the masses of the actually interacting parts of the incident and the target nucleus. The number of evaporation tracks gave some information concerning this point.

(2) The largest Castagnoli estimates (with due allowance for statistical fluctuations) of the energies of singly-charged and neutral secondary particles which interacted. Since the energy of these particles cannot be larger than the per-nucleon energy of the primary nucleus, a lower limit could be placed on the latter.

(3) The energy estimate from the emission angles θ_i of fragmentation products [Formula (3)].

(4) The distance of the maximum of the electromagnetic cascade from its origin. This distance is a rough measure of the energy of produced π^0 mesons.

All the parameters used in the estimation of the energies of the events are presented in Table V. In the last column the most likely estimate is given. Several neutron-induced interactions (1039-5, 1066-9, 1099-6) which appear in Figs. 10-12 were discarded since they gave $\log_{10} \gamma_{es}$ values which were too low to contribute to the information concerning primary energy.

B. The Angular Distributions of Particles Produced in the Collisions of Nuclei

The angular distributions of the particles produced in nucleus-nucleus collisions do not exhibit consistent features, as can be seen from Figs. 3 and 8-12. Individual

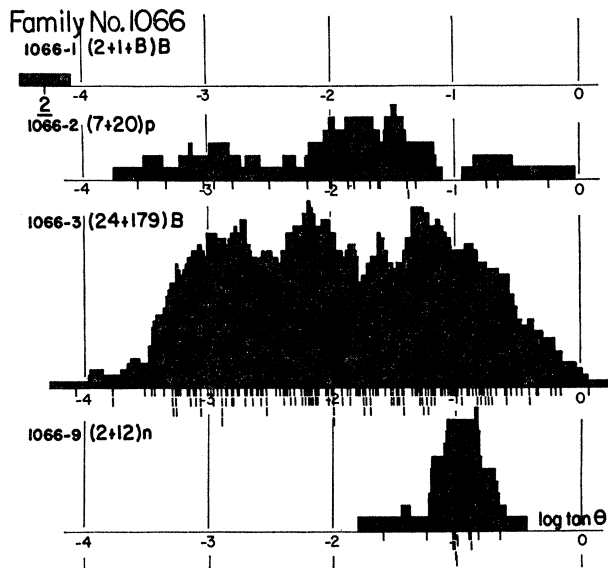


FIG. 11. $\log_{10} \tan \theta$ plot of the produced particles in the jets associated with family No. 1066.

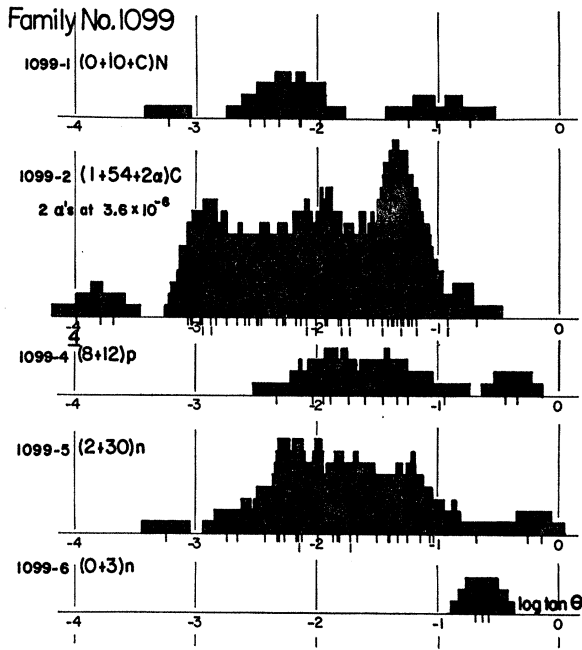


FIG. 12. $\log_{10} \tan \theta$ plot of the produced particles in the jets associated with family No. 1099.

angular distributions exhibit in a statistically significant manner a wide range of structures, but no consistent variation of the structures and σ values is observed as a function of the primary energy. These features contradict the prediction of, for example, the hydrodynamical theory according to which the angular distributions should have, within statistical fluctuations, a well-defined and unique shape (Gaussian).

It is natural, on the other hand, to expect that such a behavior be the result of the superposition, for each nucleus-nucleus interaction, of several nucleon-nucleon collisions and in part to the subsequent nuclear cascade in both the incident and the struck nuclei.

Although the shapes differ considerably, some of the angular distributions (e.g., events No. 1039-2, 1066-3, 1099-2, 1115-2) possess certain features of symmetry. Similar properties are exhibited by events described in the literature.²⁰ Once again this may be thought to reflect some kind of symmetry in the collision, where approximately equal numbers of nucleons of the incident and target nuclei may have been involved in meson production.

C. Inelasticity in the Interactions of Nuclei

The inelasticity coefficients for collisions of primary nuclei were estimated according to the relations

$$K_{ch} = \frac{1.5E_{ch}/\Delta A}{E_p}, \tag{10}$$

²⁰A. A. Loctionov and J. S. Takibaev, in *Proceedings of the International Conference on Cosmic Rays and the Earth Storm, Kyoto, 1961* (The Physical Society of Japan, Tokyo, 1962), Vol. 3, p. 412.

TABLE VI. Multiplicity and inelasticity estimates for interactions induced by nuclei.

Event No.	Type of interaction	E_p (TeV)	Estimated number of interacting nucleons ΔA	$n_s/\Delta A$	E_{ch} (TeV)	K_{ch}^a	K_γ^b
1003-1	(5+37+ α)Be	~ 4.6	≤ 4	> 9.3	2.0	> 0.16	> 0.09
1003-2	(23+95) α		4	23.7	4.1	0.34	
1005-1	(13+215)C	~ 3	12	17.9	4.7	0.20	> 0.10
1039-1	(0+24+ α) α		1	24.0	3.6	0.49	> 0.16
1039-2	(1+47) α	~ 11	3	15.6	2.4	0.11	> 0.16
1066-3	(24+179)B		11	16.3	3.0	0.30	
1099-1	(0+10+C)N	~ 14	≤ 2	≥ 5.0	0.5	> 0.02	> 0.04
1099-2	(1+54+2 α)C	~ 16	≤ 4	≥ 13.5	7.1	> 0.17	> 0.10
1115-1	(3+7+Mg)P		2	3.5			
1115-2	(11+42+Na)Mg		≤ 4	≥ 10.5			
1115-5	(0+3+Na)Na	~ 1.3	1	3.0			
1115-6	(0+51+ α +Li)Na		≤ 6	≥ 8.5			
1115-13	(1+4) α		≤ 2	≥ 2.0			
1115-20	(0+44)Li		≤ 5	≥ 8.8			

$$^a K_{ch} = (1.5E_{ch}/\Delta A)/E_p.$$

$$^b K_\gamma = (3E_\gamma/\Delta A)/E_p.$$

$$K_\gamma = \frac{3E_\gamma/\Delta A}{E_p}, \quad (11)$$

where E_{ch} is defined by Eq. (6), E_γ is the estimate of the energy transferred into γ rays from π^0 decays, and the factors 1.5 and 3 account for the π^0 component, or for the charged π component, respectively, assuming charge independence. Here ΔA refers to the number of interacting nucleons. This was taken equal to the mass number A of the primary nucleus if there were no multiply-charged fragments surviving the collision. For events in which such fragments were present, ΔA was assumed to equal the difference between the mass number of the primary nucleus and the sum of the mass numbers of the multiply-charged fragments. This gave at least an upper limit to the number of interacting nucleons of the primary nucleus.

Only very rough information concerning the inelasticity can be obtained in this way. This is because, as stated before, E_{ch} is very strongly affected by the presence of small-angle tracks and by the unknown contamination of degraded breakup protons in this angular region. The fireball-model estimate of K_{ch} [see Eq. (8)], which is not so strongly influenced by small-angle tracks, could not be used here because, in general, it is not possible for this type of interaction to separate the groups of tracks which could correspond to single fireballs. Also, E_γ obtained from the present measurements of the cascade densities gives only a lower limit to the energy carried by the π^0 mesons produced in the collision since some energy in the form of γ rays probably escaped the region in which the measurements were made. Finally, both K_{ch} and K_γ depend strongly on the number ΔA of actually interacting nucleons for which only an upper limit is known.

These estimates are presented in the last two columns of Table VI. The E_{ch} values were calculated after rejection of the smallest angle tracks, which were assumed to be breakup protons. K_γ is systematically smaller than K_{ch} , probably for the reason mentioned above. As a consequence, the K_γ values should be taken as lower limits of the inelasticity. The mean value of $\log K_{ch}$ for those events in Table VI for which the number of interacting nucleons could be estimated, corresponds to $\langle K_{ch} \rangle \gtrsim 0.25$. This value is lower than but not incompatible with the result obtained for family No. 1115. On the other hand, it is quite conceivable that even in those interactions leading to complete fragmentation of the primary nucleus, the actual number of interacting nucleons be less than the mass number A of the incident nucleus, as assumed here. Such an occurrence would increase the value obtained above for the inelasticity in the interactions of nuclei with energy in the range 1–10 TeV.

In fact, in a comparable energy interval and at even higher energies, Winn *et al.*²¹ have obtained, for nucleon-nucleus collisions in air, a median value of the elasticity

TABLE VII. Comparison of the average multiplicity for nucleon-induced collisions and the average multiplicity per interacting nucleon for nucleus-induced collisions in nuclear emulsion.^a

N_h = number of evaporation tracks	Nucleus-nucleus collisions $\langle n_s/\Delta A \rangle$ $1 \leq E_p \leq 20$ TeV	Nucleon-nucleus collisions $\langle n_s \rangle$ $0.7 \leq E_p \leq 1.4$ TeV	Nucleon-nucleus collisions $\langle n_s \rangle$ $\langle E_p \rangle \sim 0.25$ TeV
≤ 5	$\geq 8.6 \pm 1.7$	11.5 ± 3.3	10.0 ± 1.9
> 5	$\geq 17.1 \pm 1.6$	17.3 ± 5.2	16.5 ± 3.4

^a Errors are the estimated standard deviation of the distribution of the mean.

²¹ M. M. Winn, R. H. Wand, J. Ulrichs, M. H. Rathgeber, P. C. Poole, D. Nelson, C. B. A. McCusker, D. L. Jauncey, D. F. Crawford, and A. D. Bray, *Nuovo Cimento* **36**, 701 (1965).

$1-K \approx 0.54$, which is in very good agreement with our analogous data from family No. 1115. Since such determination was obtained with a technique (air shower detectors) and under experimental conditions radically different from the emulsion technique, this comparison becomes particularly significant.

4. MULTIPLICITY OF PARTICLE PRODUCTION IN NUCLEUS-NUCLEUS AND NUCLEON-NUCLEON COLLISIONS

In Table VI the data concerning the multiplicity per interacting nucleon $n_s/\Delta A$ of a primary heavy nucleus have been given. Such multiplicity shows the same dependence on N_h as observed by Rybicki;²² it is larger for events with $N_h > 5$ than for events with $N_h \leq 5$. The average multiplicities per interacting nucleon $\langle n_s/\Delta A \rangle$ for energies in the interval 1–20 TeV combined with the similar data collected by Rybicki, and the average multiplicities $\langle n_s \rangle$ obtained from our unbiased sample of nucleon interactions observed in family No. 1115 (19 interactions with energies in the interval 0.7–1.3 TeV) are given in Table VII.

Comparison of Columns 2 and 3 of this table shows that there is good consistency between the multiplicity per interacting nucleon $\langle n_s/\Delta A \rangle$ for heavy-nucleus-induced events and the average multiplicity $\langle n_s \rangle$ for nucleon-induced events for corresponding classes of interactions ($N_h \leq 5$ and $N_h > 5$). This is an additional argument for understanding the collisions of nuclei as a superposition of nucleon-nucleon collisions.

The approach of studying nucleon-nucleus interactions using a sample of nucleons from the fragmentation of heavy primary nuclei was taken in a lower energy range ($\langle E_p \rangle \approx 0.25$ TeV) by Lohrmann *et al.*⁷ The multiplicities, in particular, can be singled out and compared with the present data. This is done in Table VII where it is seen that the average nucleon-nucleus multiplicities do not exhibit appreciable differences, at least at ≈ 0.25 and ≈ 1 TeV, respectively. On the other hand, an energy dependence of the Fermi type, proportional to $E^{1/4}$ would still be statistically compatible with the data, while a dependence to $E^{1/2}$ is excluded. The ratio $\langle n_s(N_h > 5) \rangle / \langle n_s(N_h \leq 5) \rangle$ is for both experiments 1.6.

5. CONCLUSIONS

The fragmentation of heavy primary nuclei at per-nucleon energies in excess of 10^{12} eV proves to be, in favorable cases, a powerful tool for the study of an unbiased collection of nucleon-induced interactions. In the present study, essentially only one event No. 1115 induced by a $Z=15$ primary nucleus, gave a useful family of nucleon fragments; namely, a sample of 9 interactions caused by $Z=1$ fragments and 10 caused

by neutral fragments. The primary per-nucleon energy could be well established for this events as 1.3 TeV. Thus for a typical primary energy in the region of 1 TeV, the following prominent features of nucleon-induced interactions could be observed:

(a) For 17 jets ($6 \leq n_s \leq 25$) which can be interpreted as nucleon-nucleon interactions the angular distribution (in $\log_{10} \tan \theta$) of the created particles is predominantly bimodal, and inconsistent with a distribution having a rectangular shape.

(b) No asymmetry in the azimuthal distribution of the created particles could be detected in these jets. An upper limit of 1.5 BeV/c can be placed on the average transverse momentum of fireballs whose possible formation could have caused the bimodality of the angular distribution stated above in (a).

(c) The average inelasticity coefficient, as derived from the interactions of nucleon fragments is

$$\langle K_{ch} \rangle = 0.57_{-0.14}^{+0.19}.$$

(d) The average multiplicity found at $E \approx 1$ TeV, for nucleon-induced jets with $N_h \leq 5$, is $\langle n_s \rangle = 11.5 \pm 3.3$.

The main results which could be derived from the study of interactions initiated by heavy primary nuclei are:

(a) The lower limit on the average multiplicity $\langle n_s/\Delta A \rangle$ for nucleus-nucleus collisions at per nucleon energies in the region 1–20 TeV is compatible with $\langle n_s \rangle$ for nucleon-nucleus interactions at ~ 1 TeV, for both the interactions involving $N_h \leq 5$ and $N_h > 5$.

(b) The last observation together with the observation that the angular distributions are often symmetric, suggest a linear superposition in nucleus-nucleus collisions of elementary nucleon-nucleon acts of meson production.

ACKNOWLEDGMENTS

We wish to thank with deep appreciation the U. S. National Science Foundation and the U. S. Office of Naval Research for their support of this investigation and for their competent and ever willing cooperation.

The authors are indebted to Professor M. Koshiha for his significant contribution in the initial stages of this work, and to Dr. John Kidd for his help. They wish to thank R. W. Tilley for his assistance in the azimuthal symmetry analysis that involved the artificial jets.

Three of us (J. Gierula, K. Rybicki, and W. Wolter) would like to express our gratitude to Professor H. L. Anderson and the late Professor S. K. Allison for the hospitality extended to them at the Enrico Fermi Institute for Nuclear Studies and to Dr. P. Zieliński for the many discussions concerning the statistical evaluation of the data.

²² K. Rybicki, Nuovo Cimento 28, 1437 (1963).